Crack development and effect of ageing on performance of composite shell sprayed concrete tunnel linings

Jiang Su
AECOM, UK.

Alan Bloodworth
University of Warwick, UK.

ABSTRACT: Recent development and application of composite sprayed concrete lining (SCL) in major tunnelling projects have raised concerns on its short- and long-term flexural performance. Little literature has been found on the short-term crack development and the long-term ageing effect on composite SCL. Understanding of these issues will facilitate the efficient design of composite SCL. Four-point bending tests were performed on composite SCL beams to examine some aspects of these concerns. It is concluded that composite SCL beams have high residual flexural capacity; spray-applied membrane can maintain its integrity under big cracks; although the ageing effect reduces the ductility ratio of composite SCL beams in the long term, the absolute residual flexural strength increases. Conclusions drawn from the test results are compared with the current SCL tunnel design methods and the implication of differences is discussed.

1 INTRODUCTION

Sprayed concrete lined (SCL) tunnelling has seen rapid development over the last twenty years in the UK (Su 2013). Three of these developments have been the inclusion of wet-mix sprayed concrete primary lining as part of the permanent load-bearing structure, the replacement of the traditional sheet membrane between the primary and secondary linings with a spray-applied waterproofing membrane and use of a wet-mix sprayed or cast in-situ concrete secondary lining. This innovative configuration is called a composite shell lining (CSL) and has recently been adopted in projects in the UK and other Europe continent countries (Pickett 2013, Nermoen *et al*. 2011, Hasik *et al.* 2015) in soft ground with low permeability.

Due to the lack of understanding of the spray-applied membrane interface properties and data from case histories, in most cases the CSL tunnels are designed assuming an unbonded (only compressive stiffness assumed) waterproofing interface (Pickett 2013), ignoring the tensile and shear bond at the interface. In order to achieve an efficient design for CSL tunnels, research has recently been carried out mostly focusing on the following aspects: (1) the interface properties of the spray-applied membrane interface (Su & Bloodworth 2016, Holter & Geving, 2015, Holter 2015); (2) the mechanical behaviour of composite beams cut from SCL panels (Su & Bloodworth 2014, Nakashima 2015); and (3) The behaviour of a CSL tunnel when interface tension and shear bond is considered (Su & Bloodworth 2016, Su & Uhrin 2016, Pickett & Thomas 2011).

Being designed thick to minimise ground settlement in urban areas (ICE 1996), the primary lining of CSL tunnels is usually at low utilisation (Stark *et al.* 2016) and working in the pre-crack stage. Therefore, previous literature has almost exclusively focused on the lining behaviour at the pre-crack stage. Meanwhile, although some research has been carried out on the ageing effect on flexural performance of the sprayed concrete beams (Bernard 2015), no literature has been found on the long-term ageing effect on the flexural performance of CSL beams or linings. This paper presents some laboratory test results on the short- and long-term post-crack behaviour for CSL beams.

This paper will first introduce the composite mechanical behavior for CSL beams and the research methodology. The procurement of CSL beam test samples will then described, followed by the flexural test set up. The short-term post-crack behaviour of CSL beams will then be examined, focusing on the relationship between crack development, flexural capacity reduction and longitudinal strain variations. The membrane capacity to bridge different width of cracks is also commented. The third part of this paper presents four-point bending test results for beams tested 4.5 years after the cast. The evaluation of the toughness and a brief discussion on its implication are also presented. In the end, a conclusion is drawn based on the test results presented in this paper.

2 COMPOSITE MECHANICAL BEHAVIOUR

CSL beams consist of two layers of component beams, representing the primary and secondary linings, and a sandwiched layer of membrane interface. The pre-crack stress and strain distributions through the cross-section will depend on the degree of composite action, as shown in Figure 1. As this reduces from high composite to low composite, neutral axes for each component beam move away from the membrane until they reach half-depth of each component. Applying Euler-Bernoulli beam theory with an assumption of linear elastic behaviour, the lower the degree of composite action, the lower the moment (calculated from the stress blocks) for a given deformation (curvature), and hence the lower the flexural stiffness of the lining.

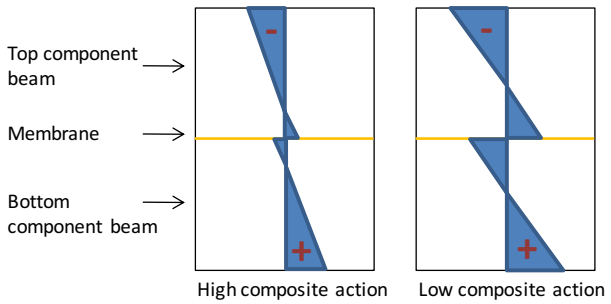

Figure 1. Typical pre-peak stress distribution for composite beam cross-section

In the latest soft ground SCL tunnel construction, steel fibre has been widely used as the main reinforcement. Neither steel bars nor steel meshes are used except at tunnel junctions and geometrically difficult locations (Su 2013). Therefore, at the post-crack stage, the steel fibres at the crack will sustain a certain amount of tensile stress. The typical post-crack stress and strain distribution through the cross section will be postulated based on laboratory test data later.

3 RESEARCH METHODOLOGY AND LABORATORY TESTS

To understand crack development and effect of ageing on performance of composite shell sprayed concrete tunnel linings, laboratory four-point bending tests on CSL beams were carried out 6 months and 4.5 years after the cast of the beams. The mid-span vertical displacement and longitudinal strains at selected positions were measured using potentiometers and strain gauges. The two sets of results were cross-examined to ensure the accuracy of the results.

3.1 *Procurement of testing samples*

Sprayed concrete wet mix specification and design are given in Tables 1 and 2 respectively. An EVA-based waterproofing membrane (TamSeal 800) was used. This product contains more than 75% by weight of EVA co-polymer, and its functional properties are expected to be similar to other EVA-based membranes. The spray was carried out at the contractor's plant facility and the direction of all spray was perpendicular to the test box (BS-EN 14487-1, 2005). After each spray, the boxes were covered with plastic sheeting to prevent exposure to sunshine or cold air, simulating a realistic environment for sprayed concrete curing in the underground. The spray was carried out during the summer (June –August 2011) in the UK, with daily temperatures ranging from 15-25 degrees Celsius. A typical CSL beam is shown in Figure 2.

Figure 2. A typical CSL beam

Table 1. Mix specification for primary and secondary lining sprayed concrete

Agg Size (mm)	Cement Type	Targeted Slump	Targeted 90-day Strength
8	CEM1	S3	40MPa

Table 2. Mix design for primary and secondary lining sprayed concrete

Materials Type	Dry Batch Weights (kg/m^3)
CEM1	450
0/4 MP Sand	1300
4/10 Gravel	550
WRA (N)	2250
Target W/C	0.45
Steel fibre	40
Accelerator	6% (weight of cement)
Superplasticiser	0.9% (weight of cement)

Samples were prepared with three alternative surface types for the primary lining substrate – as-sprayed (rough), smoothed (float finish flat surface) and regulated (smoothed by application of a regulating layer of gunite of smaller aggregate size without steel fibre. Seven composite beams, with various combinations of substrate roughness and membrane thickness, were tested as well as three pure sprayed concrete beams (Table 3). Detail of procurement of the test samples is described in Su & Bloodworth (2016).

Table 3. Dimensions of test beams

Test group	Beam Ref.	Measured membrane thickness (mm)	Substrate preparation	Thickness of top / bottom component beam (mm)
A	A1-11	4	smoothed	77 / 69
	A2-11	3	regulated	70 /77
	A3-11	3	as-sprayed	67 / 80
	A4-11	6	smoothed	69 / 75
	A5-11	10	regulated	70 / 70
	A7-11	N/A	N/A	150
B	B4-12	6	smoothed	65 / 79
	B4-13	5	smoothed	65 / 80
	B7-12	N/A	N/A	150
	B7-13	N/A	N/A	150

After transport to the University, the beams were kept in the lab under ambient temperature and humidity. Beams were tested in two groups, A and B, approximately 6 months and 54 months respectively after spray. Maximum ratio of membrane thickness to overall beam depth is 6.7% (10 mm/150 mm for beam A5-11), and maximum deviation of membrane position from half-depth is 9.3% (7 mm/75 mm for beam B4-12). Both are less than 10%, within the acceptable level of construction tolerance.

3.2 *Test setup and experimental procedure*

Test setup for Group A is shown in Figure 3. Machine loading was applied through a yellow steel crossbeam equally to two roller bearings, each on a spreader plate to distribute the loads more uniformly to the beam. One potentiometer measured vertical downward displacement of the top of the beam at midspan. Four strain gauges were attached to measure longitudinal strain, at half depth of the top and bottom component beams on each side at midspan.

In Group B the overall setup was the same but there were differences in the instrumentation. Two potentiometers were positioned at midspan, one each side of the beam top surface, to detect any component of beam torsion. The four longitudinal strain gauges were arranged to obtain more precise strain profiles through the beams, with two at half-depth of the top component beam (one each side of the beam) and the third and fourth on the top and bottom surfaces of the beam on its centreline (Figure 2). For beam B4-13, one of the strain gauges was positioned at the top ¼ of the top component beam. For all beams, machine stroke control was used with a loading rate of 0.01 mm/s to a vertical displacement of approximately 10 mm. All tests were carried out under ambient laboratory climate conditions (i.e. 15-20° in temperature and 40-60% relative humidity).

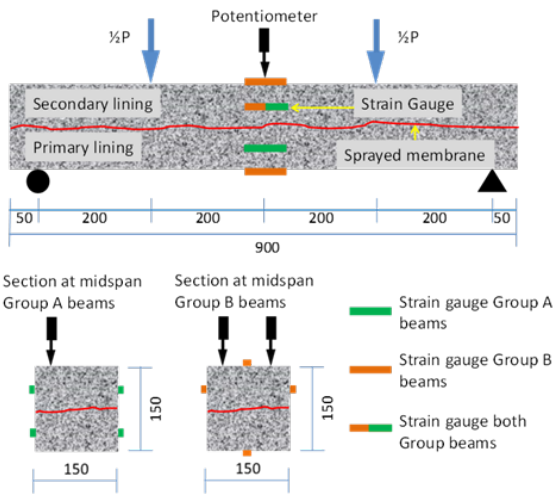

Figure 3. Flexural test set-up

3.3 *Flexural behaviour*

Load-deflection diagrams for Group A and B beams are shown in Figures 4 and 5 respectively.

For Group B beams the data is calculated from the average of the two displacements measured. A typical pattern is seen of linear behaviour up to peak load, followed by a sudden load drop and then further steady load decrease. The only major exception is beam B4-12, which has a lower and much less pronounced peak load, possibly due to unnoticed prior micro-cracking.

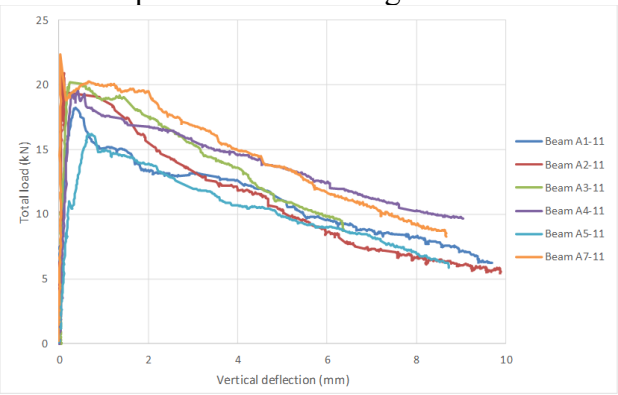

Figure 4. Load-deflection relationship for Group A beams

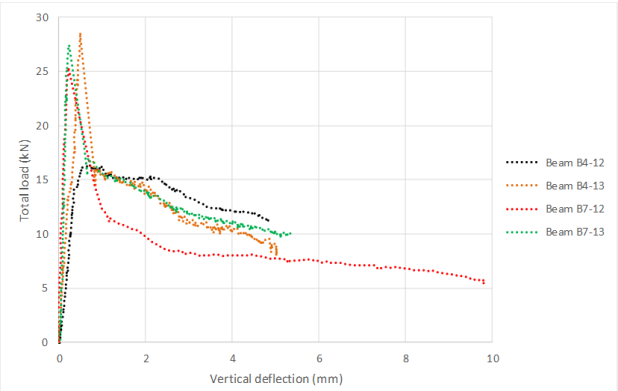

Figure 5. Load-deflection relationship for Group B beams

3.4 *Crack development*

All composite beams exhibited similar crack development. This is shown in Figure 6 for beam A2-11 and detailed as follows for that beam.

1. First visible cracking was observed when the load reached 19 kN (90% of peak load).
2. A single flexural crack was observed and was approaching the membrane when the peak load was reached.
3. With the crack having crossed the membrane and extended to ¾ of overall beam depth, the beam could still sustain 18.5 kN (88% of peak load), At crack length 80% of beam depth it could sustain 10 kN (50% of peak load).
4. Steel fibres were observed to fail in the desired pull-out mode for Group A beams but rupture for Group B beams.

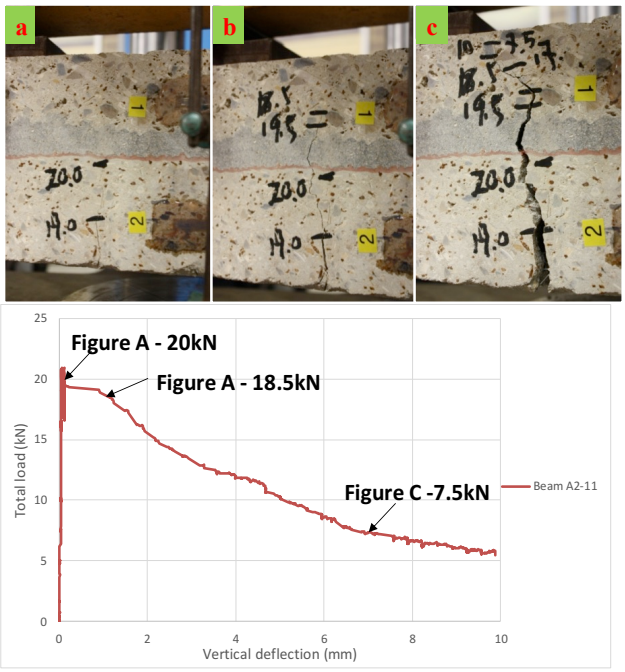

Figure 6. Crack development during the test for beam A2-11(a) approaching peak load (b) passing peak load (c) residual strength

The crack development of composite beam A2-11 is compared with that of sprayed concrete beam A7-11 in Figure 6(a). The first visible crack for sprayed concrete beam A7-11 develops when the load reached 20kN, approximately 85% of peak load (23kN).

Composite beam crack depth under 20kN is lower than for the sprayed concrete beam, which is due to a small compressive zone right below the membrane (reversing strain), as shown in Figure 2. The existence of the small compressive zone should help close the crack and thus reduce the possibility of ingress of groundwater reaching the sprayed membrane.

Figure 7. Crack development for (a) sprayed (no membrane) and (b) composite beams under indicated loadings

3.5 *Membrane crack bridging ability*

Membrane crack bridging ability is a key factor in determining the watertightness of the composite SCL tunnel lining system. It was observed and compared for composite beams with both thin and thick membrane.

Figure 6 shows the 3mm membrane in composite beam A2-11 had not broken in the post-crack region at a load of approximately 19 kN (Figure 6 (b)), but had broken by the time the load had reduced to 13 kN (Figure 6 (c)).

By contrast, Figure 8 shows the 6mm thick membrane in composite beam A4-11 had not broken in the post-crack region at a load of approximately 16 kN. The test was continued with loading reduced to 10 kN and beam vertical displacement reached 9mm. and no membrane crack was observed. This demonstrates the thick membrane has better crack bridge ability than the thin membrane and can bridge large cracks.

For soft ground SCL tunnel, the maximum allowable crack width is usually 0.3mm at the tunnel lining surface. This laboratory tests demonstrate both thin and thick membranes can bridge the crack of this scale.

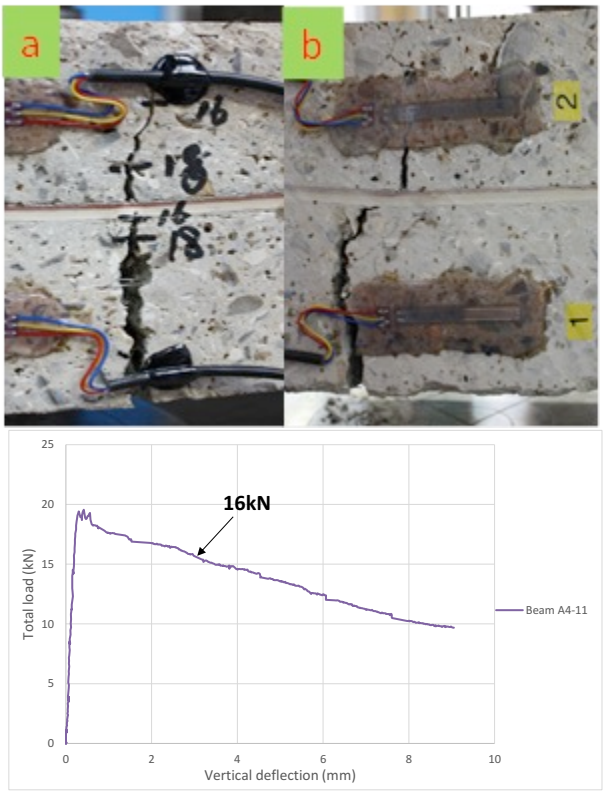

Figure 8. Crack bridging ability for composite beam A4-11with thick membrane at residual stress level

3.6 *Longitudinal strains*

Typical pre-crack longitudinal strains for beams under 50% of peak load (up to 10kN) are shown in Figure 9. It can be seen the longitudinal strains measured at half-depth of each component beam are very close in magnitude but opposite in direction. The small differences in magnitude are likely to be due to discrepancies between the top and bottom component beam thickness.

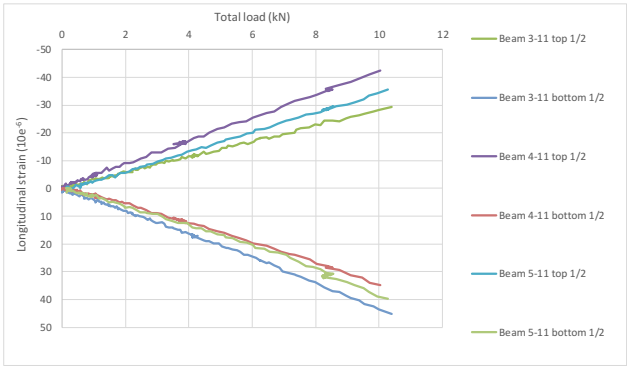

Figure 9. Typical pre-peak longitudinal strains for composite beams A3-11, A4-11 and A5-11.

Pre- and post-crack longitudinal strains for composite beam B4-13 are shown in Figure 10. Three measurements were made for the top component beam at top surface, ¼ and ½ depth of the component beam from the top. It can be found that:

1. Maximum flexural tensile strain for a composite sprayed concrete beam can be more than 200 microstrain.
2. Reversible strain on unloading can be extrapolated for the top component beam based on its three strain readings.
3. At the post-crack stage, the strain at the bottom goes back down the same path after the cracking, showing the steel fibres were taking less and less load during the pulled-out process.
4. The strain at the top surface level is much larger post-crack than pre-crack under the same loading.
5. The strain at the upper ¼ depth of top component beam is slightly larger post-crack than pre-crack under the same loading.
6. The strain at the half depth of top component beam is almost the same for the pre- and post-crack under the same loading.

The reason for these observations will be explained in next section.

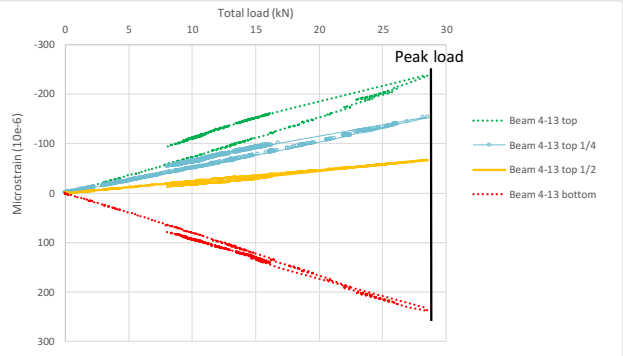

Figure 10. Typical pre- and post-peak longitudinal strains for composite beams B4-13.

3.7 *Post-crack stress at cross-section*

Based on the longitudinal strain data obtained from laboratory tests, the post-crack stress diagram for a composite beam is postulated, as shown in Figure 11, with the crack shown as the red triangle.

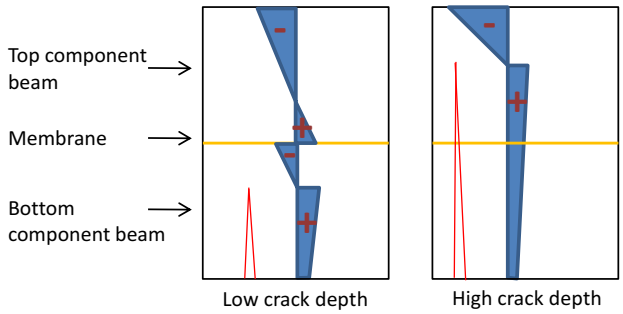

Figure 11. Post-crack stress diagram derived from longitudinal strain data

For the low crack depth scenario (i.e. crack not reaching the membrane), residual tensile stress sustained by the steel fibres is shown for the whole crack depth, above which is a pair of compression and tension zones of triangular shape below and above the membrane interface. Due to the occurrence of the crack, moving up of the neutral axis and more deflection for the CSL beam post-crack than pre-crack under the same loading, the two triangular compression and tension zones will be smaller in depth, leading to a compression zone at the upper part of the top component beam larger in both depth and maximum strain value at the top surface in comparison to the pre-crack scenario. This explains why the compressive strain at the top surface of the top component beam is larger for post-crack path than for pre-crack path under the same loading.

For the high crack depth scenario (i.e. crack beyond the membrane), residual tensile stress sustained by the steel fibres is again shown for the whole crack depth, up to the top component beam. Therefore, strain reversing will occur only at the top component beam, with a neutral axis at the crack tip. Thus, the compression zone at the upper part of the top component beam will be smaller in depth but much bigger in the maximum strain value in comparison to the pre-crack strain diagram.

4 EFFECT OF AGEING

4.1 *Ageing effect on flexural behaviour*

From the load-deflection relationships for the three sprayed concrete beams (Figure 11), the Group B beams (B7-12 & B7-13), tested 4.5 years after spray, have higher peak load but lower residual strength than the Group A beam (A7-11), tested six months after spray. Examination of the cracked cross-sections showed different failure modes for the fibres, with those in the Group A beam failed by pull-out, but by rupture in the Group B beams. This agrees with the experience of Bernard (2015), who tested fibre reinforced sprayed concrete beams at ages from one to five years and found that concrete hardening with age changed the failure mechanism from desirable fibre pull-out to fibre rupture.

Comparing Figures 4, 5 and 11 shows the Group B beams have a much higher and more pronounced peak strength than Group A beams but similar post-peak residual strength, which means a much steeper decline after peak stress compared to the Group A beams. The implication of this phenomenon is discussed in the next section.

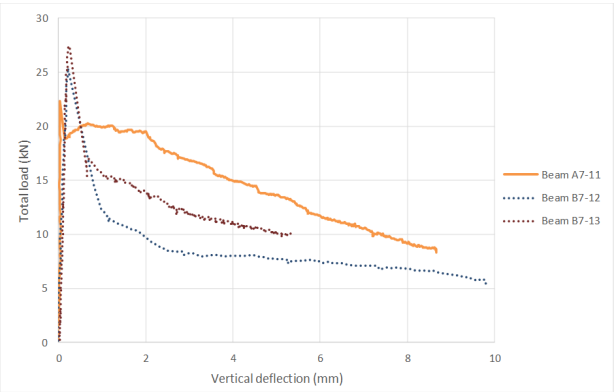

Figure 12. Load-deflection relationships for all pure sprayed concrete beams

4.2 *Evaluation of toughness*

Historically, most fibre-reinforced SCL was used in rock tunnels, where lining performance criteria in most standards focuses on the large deformation stage, whereas in soft ground SCL tunnelling small deformations are desired.

The performance of fibre reinforced SCL was traditionally evaluated by post-peak toughness, which may be expressed either in terms of energy-, strength- or deflection-based dimensionless indices (Gopalaratnam & Gettu 1995), all of which were developed for fibre-reinforced SCL tunnels in rock. Energy-based indices have been widely used in countries such as Norway (Norwegian Concrete Association 2011) and Australia (Concrete Institute of Australia 2010), where thin SCL tunnel linings are used together with bolts in blocky or unstable ground, requiring a high degree of ductility and energy absorption over a significant deflection range. In contrast, strength-based indices are used in countries like the UK (ICE 1996) and Germany (RILEM 2003) where thicker SCL is used in soft ground, subjected to relatively small flexural deformation. They have the advantage of a relatively simple test configuration for their determination compared to energy-based methods (a beam compared to a round panel). The third design method using deflection-based indices (Ward and Li 1990) needs further development before practical application. This section examines whether strength based indices, which were derived purposely for rock tunnels, are best suitable for soft ground SCL tunnel design.

For fibre-reinforced SCL tunnels in any ground conditions, there are usually two major considerations on toughness: (a) maintaining certain strengths at ULS and SLS stages and (b) achieving the desired pull-out fibre failure mechanism, avoiding fibre rupture. The former can be realised by specifying minimum flexural strength at a particular deflection (or equivalent crack width) for beams under four-point bending, and the latter by specifying strength ratio at different post-peak deflections. Model Code (2010) adopts both principles and evaluates toughness from the absolute value of f_{R1} and ratio between f_{R1} and f_{R3}, the tensile stresses at the bottom of the beam at 0.75 mm and 3.0 mm central deflection respectively in beam tests according to BS EN 14488-3:2006 (BSI 2006) and ASTM A820/820M (ASTM 2011). The f_{R1} class is determined as the stress value at the lower end of a range in which the test result fails, and the f_{R3}/f_{R1} ratio is similarly classified by a letter denoting the range within which the ratio sits, as described in Table 2. The overall strength class of a beam is thus denoted by a number followed by a letter. This assessment methodology is applied to the composite beams in this study with the results given in Table 3, although it should be noted that these are not directly comparable to tests according to the aforementioned standards because the beam dimensions are slightly different.

Table 4. Mix specification for sprayed concrete lining

Class items	Class criteria
f_{R1} class (MPa)	1.0; 1.5; 2.0; 2.5; 3.0; 4.0; 5.0; 6.0; 7.0; 8.0;
$f_{R3/fR1}$ ratio	"a" if $0.5 \leq f_{R3}/f_{R1} \leq 0.7$; "b" if $0.7 \leq f_{R3}/f_{R1} \leq 0.9$; "c" if $0.9 \leq f_{R3}/f_{R1} \leq 1.1$; "d" if $1.1 \leq f_{R3}/f_{R1} \leq 1.3$; "e" if $1.3 \leq f_{R3}/f_{R1}$;

Table 5 shows little variation in strength class over the Group A and B beams, which all lie within the range 2.5a to 3.0b. Thus this assessment method for toughness has not reflected the impact of ageing causing a more pronounced peak stress but steeper stress reduction after peak stress, together with fibre rupture. This is because this strength method was developed mainly for rock SCL tunnels and thus focuses on post-peak strength behaviour after 0.75mm deflection, deriving the strength class based only on f_{R1} and f_{R3}. For soft ground SCL tunnels, the lining is normally designed in its pre-peak state, and it is more pertinent to examine the ratio between f_{R1} and the peak stress f_T, shown in the last column in Table 3. This ratio is above 0.85 for all Group A beams, but on the contrary less than or equal to 0.60 for Group B beams (except for B4-12 which is an outlier as discussed earlier), and hence is able to distinguish the effect of ageing in Group B beams in comparison to Group A beams, unlike the established strength method based on f_{R3}/f_{R1}. The normalized load-deflection relationships for all tested beams (Group A beams tested 6 months after the cast and Group B beams tested 4.5 years after the cast) are shown in Figure 13.

Table 5. Key lining performance parameters, derived ratios and strength class (MPa)

Beam Ref	f_T	f_{R1}	f_{R3}	f_{R3}/f_{R1}	Strength Class	f_{R1}/f_T
A1-11	3.2	2.77	13.18	0.84	2.5b	0.85
A2-11	3.7	3.40	12.87	0.68	3.0a	0.91
A3-11	3.6	3.43	15.3	0.79	3.0b	0.96
A4-11	3.4	3.20	15.69	0.87	3.0b	0.92
A5-11	2.9	2.63	11.97	0.80	2.5b	0.92
A7-11	4.0	3.58	16.83	0.84	3.0b	0.91
B4-12*	2.9	2.84	13.25	0.82	2.5b	0.98
B4-13	2.1	2.99	10.96	0.65	2.5a	0.60
B7-12	4.5	2.56	8.27	0.57	2.5a	0.57
B7-13	4.9	2.95	11.99	0.73	2.5b	0.60

*Unusual data possibly due to micro-cracking damage prior to test

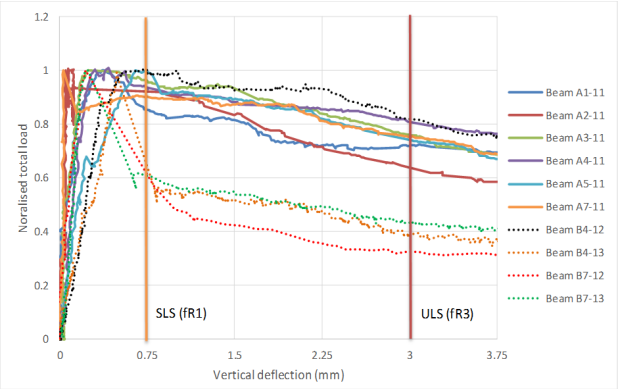

Figure 13. Normalised load-deflection relationships for all beams

4.3 *Discussion on ageing effect*

Essentially, the ratio f_{R3}/f_{R1} expresses the rate of reduction of tensile capacity between small (0.75 mm) and large (3.0 mm) deflections, whilst f_{R1}/f_T reflects the rate of reduction between peak stress and small deflection. From designers' perspective, the ideal performance of a soft ground SCL is linear elastic perfectly plastic, with both ratios equal to 1.0 and providing the most effective use of material. For Group B beams, although the residual tensile strengths f_{R1} and f_{R3} are similar to Group A beams, their peak strengths are much higher so that their ratios f_{R1}/f_T are much lower than for Group A beams. Because the residual rather than the peak stress is normally used in lining ultimate limit stage (ULS) design for sprayed concrete flexural tensile strain up to 2.5% (Pickett & Thomas 2011), a SCL with a very high peak but moderate residual flexural stress is strictly speaking a waste of material. Thus the ratio f_{R1}/f_T is fundamentally more a material efficiency rather than ductility or strength index like f_{R3}/f_{R1}, and hence represents the current trend towards more sustainable design and construction in the industry. The ratio f_{R1}/f_T may be maximised and hence an economical and sustainable SCL mix design achieved by means of a combination of moderate strength of both sprayed concrete and fibres. This shall achieve post-crack strength and ductility no lower than an SCL mix using only either high strength concrete or steel fibres.

There is a possibility in the future that with further increases in achievable concrete compressive strength, the fibre rupture failure mechanism will become more pronounced once the concrete has aged, leading to lower residual strengths f_{R1} and f_{R3} whilst not necessarily changing the ratio f_{R3}/f_{R1}. This raises concern as to whether flexural strength and strength class measurements made in the short term are conservative or not for a structure with a design life more than 100 years.

5 CONCLUSION

A series of laboratory tests have been carried out on fibre-reinforced sprayed concrete beams with sandwiched spray-applied waterproofing layer, representing elements of a CSL tunnel lining. The following conclusions can be drawn from this research.

1. The tests under ambient laboratory climate conditions showed clear evidence of a certain degree of (although not full) composite mechanical behaviour from measured deflections and strains both pre-crack and post-crack.
2. Beams failed by growth of a single crack at midspan, and showed significant plateaus of residual stress after peak load.
3. Reversible strain distributions were observed in composite beams during the pre-crack stage and post-crack small crack scenario.
4. A thick membrane can bridge larger crack width than the thin membrane.
5. The ageing effect on sprayed concrete and composite beam resulted in a change of failure mechanism for steel fibres and a reduction of the ratio between the small crack stress and the peak stress.
6. The current beam robustness evaluation method does not reflect the ageing effect on the residual flexural capacity for CSL tunnel linings in soft ground.
7. An economical and sustainable SCL mix design should be achieved by means of a

combination of moderate strength of both sprayed concrete and fibres. This shall achieve post-crack strength and ductility not lower than SCL only using either high strength concrete or steel fibres.

ACKNOWLEDGEMENTS

The authors would like to express their thanks to Mott MacDonald and Normet for their financial support of the research.

REFERENCES

ASTM A820/A820M-11. 2011. *Standard Specification for Steel Fibers for Fiber-Reinforced Concrete*. ASTM International, West Conshohocken, PA, 4 p.

Bernard, E. 2015. *Age-dependent changes in post-crack performance of fibre reinforced shotcrete linings*. Tunnelling and Underground Space Technology 49: 241-248.

BSI. 2006. *BS EN 14488-3:2006 Testing Sprayed Concrete – Part 3: Flexural strengths (first peak, ultimate and residual) of fibre reinforced beam specimens*. London, 12 p.

Concrete Institute of Australia. 2010. *Shotcreting in Australia: Recommended Practice, 2nd ed*. 84 p.

Fib. 2010. *Model Code 2010—First Complete Draft*. fib Bulletin, (55), 318 p.

Gopalaratnam, V.S., Gettu, R. 1995. *On the characterization of flexural toughness in fiber reinforced concretes.* Cement and concrete composites. 17 (3), 239-54.

Hasik, O., Junek, J., Zamecnik, M. 2015. *Metro Prague – use of sprayed waterproofing membrane in deep level station*. In: proceedings of the ITA/AITES World Tunnel Congress, 2015, Dubrovnik, Croatia.

Holter, K.G., Geving, S., 2015. *Moisture transport through sprayed concrete tunnel linings*. Rock Mech. Rock Eng. 49(1), 243-272.

Holter, K.G., 2016. *Performance of EVA-Based Membranes for SCL in Hard Rock. Rock Mechanics and Rock Engineering*, 49 (4), 1329-1358.

ICE. 1996. *Sprayed Concrete Linings (NATM) for Tunnels in Soft Ground: Design and Practice Guide (ICE design and practice guides)*. London: Telford. 96 p.

Nakashima, M., Hammer, A.L., Thewes, M., Elshafie, M., Soga, K. 2015. *Mechanical behaviour of a sprayed concrete lining isolated by a sprayed waterproofing membrane*. Tunnelling and Underground Space Technology 47: 143-152.

Nermoen, B., Grøv, E., Holter, K.G., Vassenden, S. 2011. *Permanent waterproof tunnel lining based on sprayed concrete and spray-applied double-bonded membrane. First Norwegian experiences with testing under freezing conditions, design and construction*. In: Proceedings of 6th international symposium on sprayed concrete. Tromso, Norway.

Norwegian Concrete Association's Publication no. 7. 2011. *Sprayed concrete for rock support*.

Pickett, A., Thomas, A.H. 2011. *The design of composite shell linings*. In: Proceedings of the 6th International Symposium on Sprayed Concrete, Tromso, Norway, pp 402–413.

Pickett, A. 2013. *Crossrail sprayed concrete linings design*. In: Underground. The Way to the Future. Proceedings of World Tunnel Congress 2013. Abingdon, GB, CRC Press, pp 956-963.

RILEM TC 162-TDF 2003.*Test and design methods for steel fibre reinforced concrete. σ-ε-design method, final recommendation*. Materials and Structures. 36 (8), 560-567.

Stark, A., Rangel, L., Wade, C. 2016. *Analyses of convergence and utilization of SCL tunnels during excavation*. In. Crossrail Project Infrastructure Design and Construction volume 3. London, GB, ICE Publishing; pp 89-104.

Su, J. 2013. *Design of sprayed concrete lining in soft ground – a UK perspective*. In: Underground. The Way to the Future. Proceedings of World Tunnel Congress 2013. Abingdon, GB, CRC Press; 2013, pp 593-600.

Su, J., Bloodworth, A. 2014. *Experimental and numerical investigation of composite action in composite shell linings*. In: Proceedings of 7th international symposium on sprayed concrete, Sandefjord, Norway.

Su. J., Bloodworth, A. 2016. *Utilizing composite action to achieve lining thickness efficiency for sprayed concrete lined (SCL) tunnels*. In: Proceedings of World Tunnelling Congress 2016. San Francisco, USA.

Su. J., Uhrin. M. 2016. *Primary-secondary lining interactions for composite sprayed concrete lined tunnels using sprayed waterproofing membrane.* In: Proceedings of World Tunnelling Congress 2016. San Francisco, USA.

Su. J., Bloodworth, A. 2016. *Interface parameters of composite sprayed concrete linings with spray-applied waterproofing*. Tunnelling and Underground Space Technology 59, 170-182.

Ward, R.J., Li, V.C. 1990. Dependence of flexural behaviour of fiber reinforced mortar on material fracture resistance and bean size. AC1 Mater J., 1990. 87(6) 627-637.